ACS Combinatorial Science

Research Article

pubs.acs.org/acscombsci

Focused Fluorescent Probe Library for Metal Cations and Biological Anions

Hyun-Woo Rhee,[†] Sang Wook Lee,[†] Jun-Seok Lee,[§] Young-Tae Chang,*[,§] and Jong-In Hong*[,†]

[†]Department of Chemistry, Seoul National University, Seoul 151-747, Korea

[§]Department of Chemistry, National University of Singapore, 3 Science Drive 3, Singapore 117543, Republic of Singapore

Supporting Information

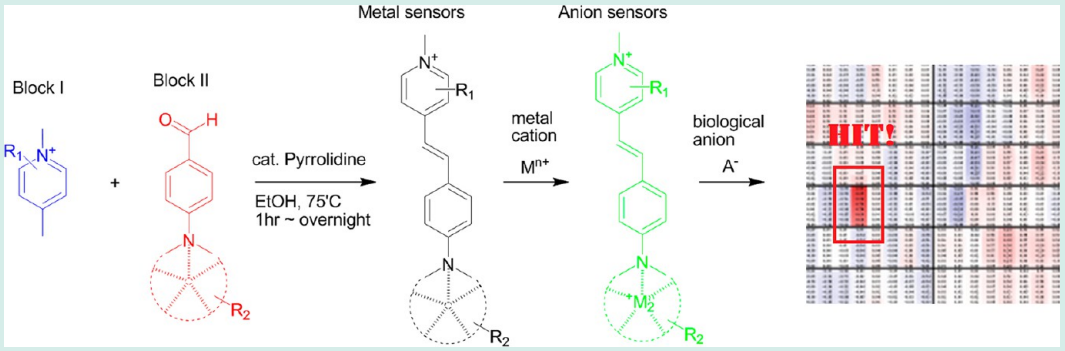

ABSTRACT: A focused fluorescent probe library for metal cations was developed by combining metal chelators and picolinium/quinolinium moieties as combinatorial blocks connected through a styryl group. Furthermore, metal complexes derived from metal chelators having high binding affinities for metal cations were used to construct a focused probe library for phosphorylated biomolecules. More than 250 fluorescent probes were screened for identifying an ultraselective probe for dTTP.

KEYWORDS: *fluorescent probe library, metal cations, biological anions, thymidine*

Fluorescent probes have been widely used for molecular cellular biology research, disease diagnosis, and environmental pollution detection.[1] The selectivity of a probe is the most important factor in the detection of a specific target among a myriad of analytes. In particular, the detection of a specific phosphorylated biomolecule is challenging because there are a large number of important phosphorylated biomolecules in cells.[2] It is a formidable task to design ultraselective probes that show distinct fluorescent signals for specific analytes because current molecular modeling technology cannot predict both the structure of a probe−analyte complex and the fluorescence signal change upon binding. Recently reported ultraselective probes were developed serendipitously in the course of screening various analytes.[3]

The bis(Zn^{2+}-2,2′-dipicolylamine) complex has been widely used for the detection of phosphorylated biomolecules among various anions.[4,5] However, because of its strong binding affinity for oligophosphate groups, probes using the bis(Zn^{2+}-2,2′-dipicolylamine) complex as a binding agent cannot perfectly distinguish (deoxyribo)nucleotide triphosphates (dNTPs and NTPs) from pyrophosphate (PPi) or other phosphate-containing biomolecules.[4,5] Therefore, a new molecular receptor or probe is required for the selective detection of dNTP or NTP from among other phosphorylated biomolecules.

Recently, the diversity-oriented fluorescence library approach has shown promise for the detection of various biomolecules.[1g,6] Because it is rather laborious to develop ultraselective probes by synthesizing and screening thousands of fluorescent molecules, we thought that a supramolecular approach to a focused library would minimize the size of the library and increasing the chance of success. Our approach involves the use of molecular receptors as synthetic blocks in the combinatorial synthesis of fluorescent probes for a target molecule.

Herein, we demonstrate the effectiveness of a focused library comprising metal chelators and styryl-based fluorescent dyes in providing ultraselective probes for the detection of metal ions and 2′-deoxythymidine triphosphate (dTTP). We chose styryl-based fluorescent dyes as signaling units because of the following advantages. First, their synthesis is simple; a single condensation reaction between picolinium/quinolinium blocks and benzaldehyde receptor blocks yields the desired dyes (Figure 1). Second, all styryl-based dyes are supposed to have a fully conjugated fluorophore structure with a metal ion receptor. Thus, their fluorescence is sensitive to proper binding with a specific metal cation through the intramolecular charge transfer (ICT) mechanism.[3b,7] Third, the styryl dye has an intrinsic large Stokes shift (>100 nm) and a positive net charge, which enhances its solubility in water.

Received: March 19, 2013
Revised: June 18, 2013
Published: August 15, 2013

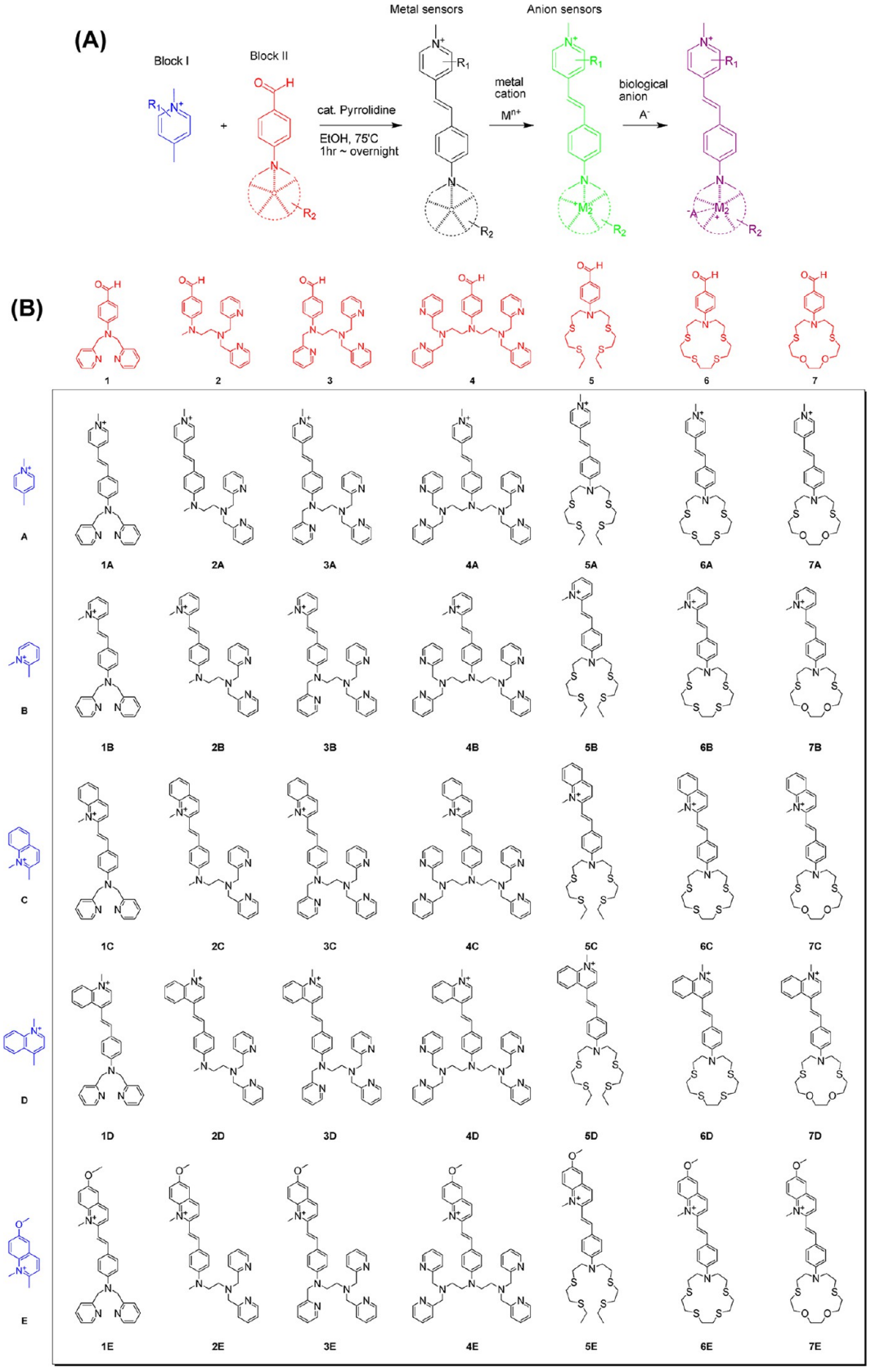

Figure 1. (A) Schematic strategy of combinatorial synthesis for fluorescent probes. Styryl-based ligands were used for metal cation sensing and metal chelated styryl-based ligands for biological anion sensing. (B) Building blocks for synthesis of styryl-based ligands and structures of synthesized 35 styryl-based ligands.

dx.doi.org/10.1021/co400034x | *ACS Comb. Sci.* 2013, 15, 483−490

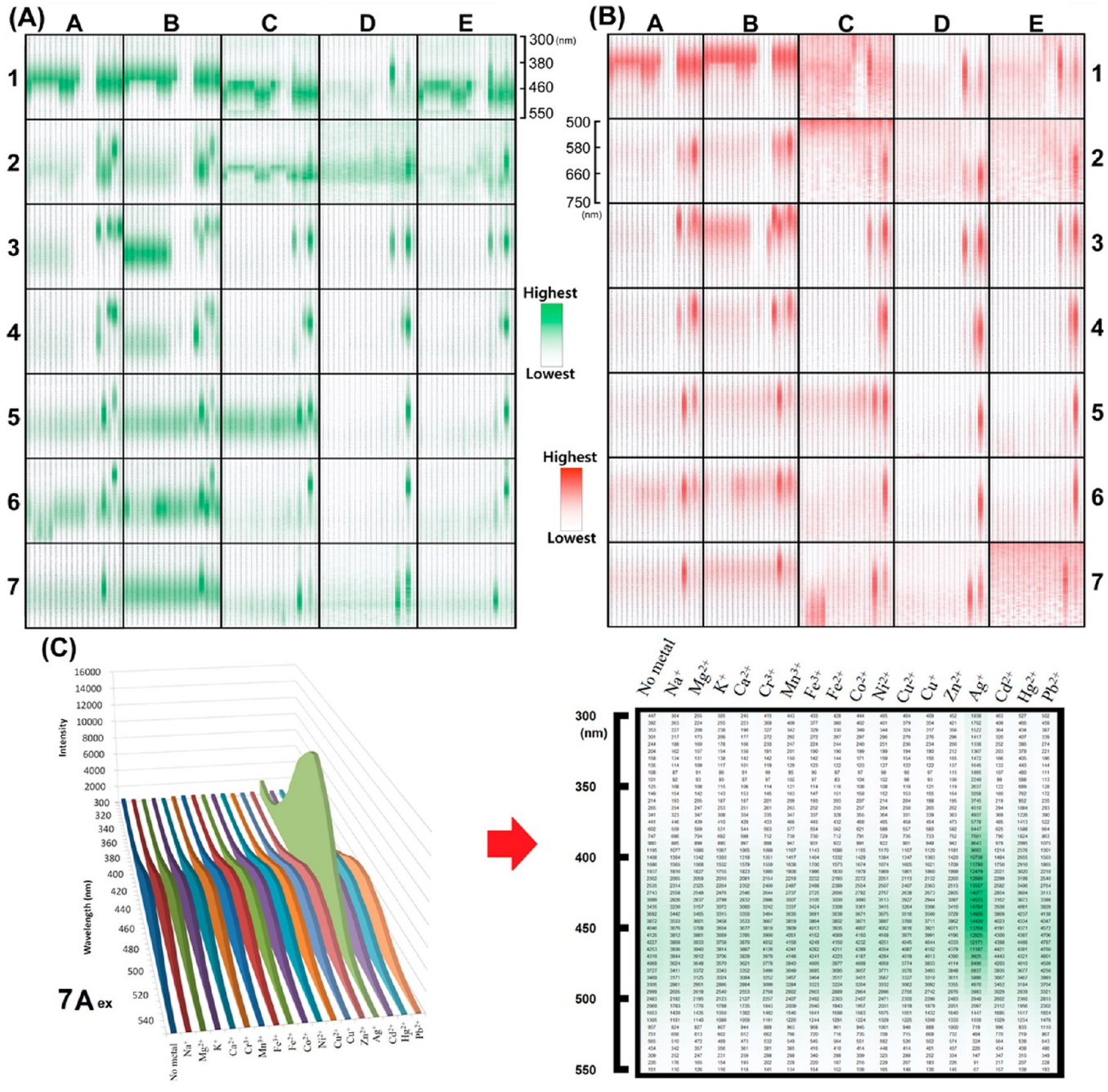

Figure 2. Primary screening of metal cations (from left column to right: no metal cation, Na^+, Mg^{2+}, K^+, Ca^{2+}; each 100 mM. Cr^{3+}, Mn^{3+}, Fe^{3+}, Fe^{2+}, Co^{2+}, Ni^{2+}, Cu^{2+}, Cu^+, Zn^{2+}, Ag^+, Cd^{2+}, Hg^{2+}, Pb^{2+}; each 50 μM.) against metal ion probes (each 5 μM). (A) Metal cation-induced excitation spectrum changes of 35 fluorescent probes: 300−550 nm. λ_{em} = 580 nm. (B) Metal cation-induced emission spectrum changes of 35 fluorescent probes = 500−750 nm. λ_{ex} = 400 nm. The intensities of fluorescence spectra are converted to the false-color intensities; green color intensity was used for the excitation spectrum and red color intensity was used for the emission spectrum. (C) Detailed view of the excitation fluorescence spectrum changes of probe **7A** upon addition of various metal cations (left) and its false-color intensity image (right) for a simple view. The highest and lowest values of the fluorescence intensity were determined from the total titration values for each probe. Metal cation screening experiments were performed in HEPES buffer solution (10 mM, pH 7.4, 25 °C). See SI for the expanded version.

Each of the 5 picolinium/quinolinium blocks (**A**−**E**) and 7 receptor blocks (**1**−**7**) was prepared in a few steps (see the Supporting Information (SI) for detailed experimental procedures). Receptor block groups have a 2,2′-dipicolylamine moiety (**1**, **2**, **3**, **4**)[1b,3a,4,5,8] or an azathia crown ether unit (**5**, **6**, **7**).[9] Using these building blocks, 35 metal ion probes were efficiently synthesized through the Knoevenagel condensation reaction (Figure 1).The products were purified by silica gel column chromatography and prep-HPLC, and they were characterized by ^{1}H and ^{13}C NMR and high-resolution mass data (see SI). The probes showed varied fluorescence emission wavelengths, ranging from 540 to 675 nm (λ_{ex} = 400 nm), with the more conjugated and para-*N*-methyl-substituted products at the longer wavelengths (see SI).

We initially screened each probe (5 μM) against 17 metal cations, including the four most abundant in human body (Na^+, K^+, Mg^{2+}, and Ca^{2+}) and 13 others (Zn^{2+}, Cd^{2+}, Hg^{2+}, Ag^+, Cu^{2+}, Cu^+, Fe^{3+}, Fe^{2+}, Cr^{3+}, Mn^{2+}, Co^{2+}, Pb^{2+}, and Ni^{2+}) known

dx.doi.org/10.1021/co400034x | *ACS Comb. Sci.* 2013, 15, 483−490

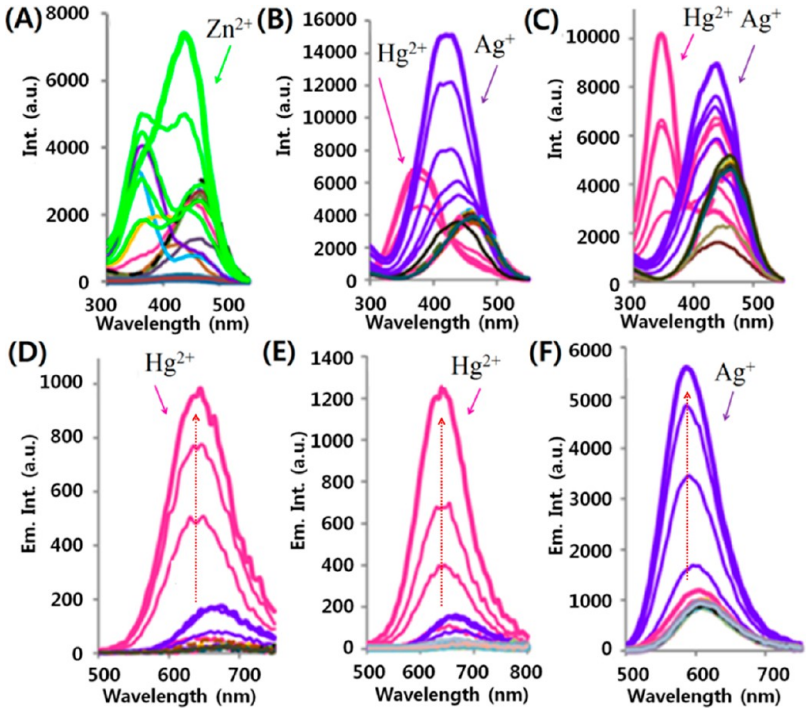

Figure 3. Fluorescence titration spectra of the selected probes (each 5 μM) for metal cations: excitation spectra (ex. spec.) changes (A, B, and C, *x*-axis = wavelength, *y*-axis = emission intensity) and emission spectra (em. spec.) changes (D, E, and F, *x*-axis = wavelength, *y*-axis = emission intensity) for each probe. Spectra changes of the probe upon addition of metal ions were represented with different colors (Zn^{2+} (green), Hg^{2+} (pink), Ag^{+} (deep purple), Cd^{2+} (sky blue), Pb^{2+} (yellow), and without metal cation (black)). (A) **4B**, Zn^{2+} (1, 2, 5, 10, 20 μM), Hg^{2+}, Cd^{2+}, Pb^{2+}, and Ag^{+} (each 50 μM), other metal cations (each 50 μM); (B) **5A**, Hg^{2+} or Ag^{+} (each 1, 2, 5, 7, and 10 μM), other metal cations (each 50 μM); (C) **6A**, Hg^{2+} or Ag^{+} (each 5, 7, 10, 20, and 50 μM), other metal cations (each 50 μM); (D) **5D**, Hg^{2+} or Ag^{+} (each 2, 5, 10, and 20 μM), other metal cations (each 50 μM); (E) **6D**, Hg^{2+} or Ag^{+} (each 5, 10, 20, and 50 μM), other metal cations (each 50 μM); and (F) **7A**, Hg^{2+} or Ag^{+} (each 5, 7, 10, and 20 μM), other metal cations (each 50 μM). Other metal cations (Mn^{2+}, Cr^{3+}, Fe^{3+}, Fe^{2+}, Cu^{2+}, Co^{2+}, Ni^{2+}, and Cu^{+}) that did not show significant changes were depicted with various colors. These spectra were recorded in HEPES buffer solution (10 mM, pH 7.4, 25 °C). Emission and excitation spectra were collected at fixed excitation and emission wavelengths, 400 and 580 nm, respectively. See SI for details.

to play essential roles or exhibit toxicity.[10] We collected both the fluorescence excitation and emission spectra at fixed emission (580 nm) or excitation wavelengths (400 nm) for easy comparison of data. As expected, all the probes showed fluorescent responses (turn-on, turn-off, or fluorescence shift) when the metal cations were added (Figure 2).

Primary screening led to the identification of several probes that are specific to certain metal cations. The selectivity of the probes for the metal cations was confirmed by performing titration experiments with metal ions of various concentrations (0, 2, 5, 10, 20, 50 μM). As shown in Figure 3, the fluorescence spectral changes of the selected probes for specific metal cations (Zn^{2+}, Ag^{+}, Hg^{2+}) were classified into two types: fluorescence excitation titration spectra (Figures 3A, B, and C) and fluorescence emission titration spectra (Figures 3D, E, and F). For example, in Figure 3A, the wavelength of maximum emission of excitation spectra of **4B** was gradually shifted with an increase in the concentration of Zn^{2+} ions. Similarly, in the case of **5A** and **6A**, blue-shifted excitation spectra with an increase in the emission intensity were obtained upon the increasing addition of Ag^{+} or Hg^{2+} ions (Figures 3B and C). Interestingly, **5D** and **6D** displayed a gradual increase in the emission intensity with the concentration of Hg^{2+} ions (Figures 3D and E). However, **7A** revealed a selective response to Ag^{+} ions with an increase in the emission intensity (Figure 3F). These probes (**4B**, **5A**, **6A**, **5D**, **6D**, and **7A**) were identified as ultraselective probes for specific metal cations (Zn^{2+}, Ag^{+} and Hg^{2+}). In some cases, the binding affinities (SI Table S1) of probes to specific metal cations are very strong (K_d values in nanomolar to picomolar ranges). It is noteworthy that despite having the same receptor unit, probes (e.g., **5A** vs **5D**, see SI Figure S8) show different degrees of fluorescence enhancement. These metal ion probes did not show significant fluorescence response to pH changes (pH 6−8) in a physiological condition due to low pK_a values of amine of the aniline-based receptors (see SI Figure S9). **6A** was successfully utilized for selective cellular imaging of Hg^{2+} (SI Figure S10).

These results indicated that metal ion probes from the **2** to **7** series can bind to specific metal cations (Zn^{2+}, Ag^{+}, Cd^{2+}, Hg^{2+}, and Pb^{2+}) with binding affinities in the range 10^{5}−10^{11} M^{-1} (K_a values, see SI Table S1). Therefore, a majority of the mixtures of these metal cations (10 μM) with each of these metal ion probes (10 μM) resulted in a large degree of binding. Such interactions can in turn be used as probes for biological anions because anion−metal binding affects metal−receptor coordination, resulting in a observable fluorescence changes (shift, turn-on/turn-off).[4,5,11]

Over 250 anion probes were prepared by the addition of 1 equiv of each of 11 metal cations (Zn^{2+}, Ag^{+}, Cd^{2+}, Hg^{2+}, Pb^{2+}, Mn^{2+}, Fe^{3+}, Fe^{2+}, Cu^{2+}, Co^{2+}, and Ni^{2+}) to each of the 24 metal cation probes (10 μM, pH 7.4, 10 mM HEPES solution) (Figure 4). Series **1** compounds were excluded because of low metal binding affinity and series **E** probes were excluded because of low fluorescence quantum yield. Seven phosphorylated nucleotides (dATP, dCTP, dGTP, dTTP, ATP, ADP, and AMP), and PPi were screened against this probe library.

dx.doi.org/10.1021/co400034x | *ACS Comb. Sci.* 2013, 15, 483−490

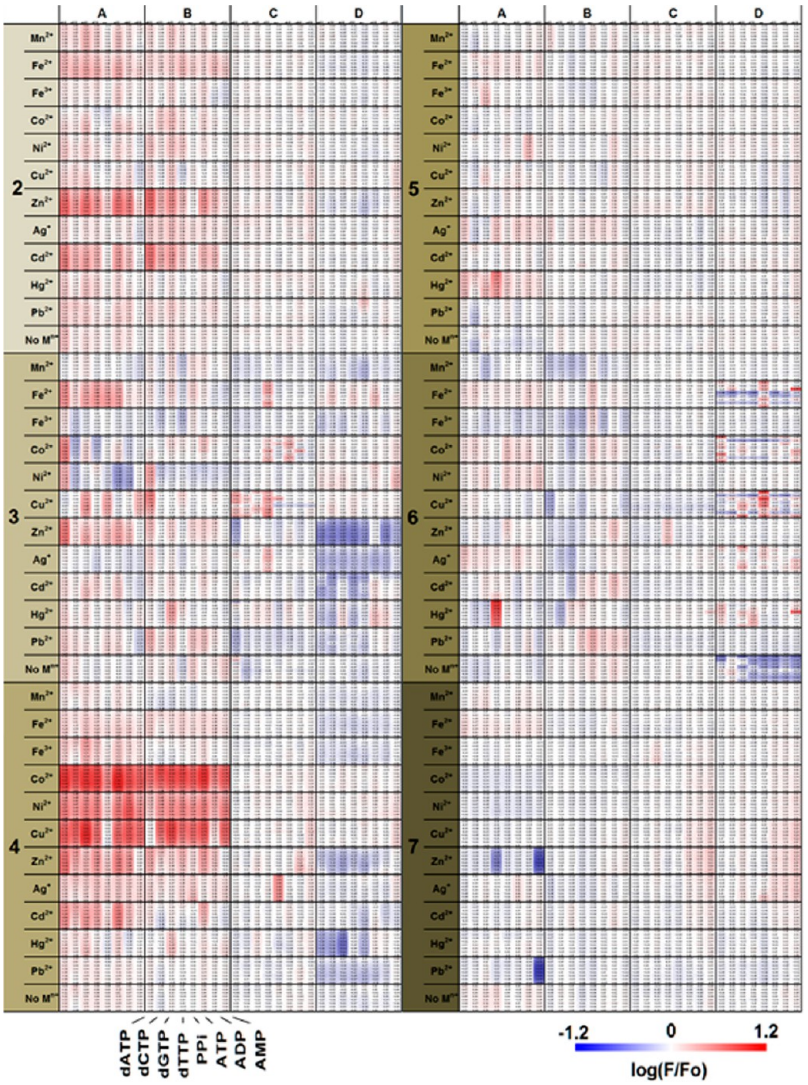

Figure 4. Primary screening heat map for biological anions (dATP, dCTP, dGTP, dTTP, PPi, ATP, ADP, and AMP; each 100 μM, 10 mM HEPES buffer, pH 7.4, 25 °C) against 264 anion probes, which consist of 24 metal ion probes (each 10 μM) and 1 eq of 11 metal cations (Mn^{3+}, Fe^{3+}, Fe^{2+}, Co^{2+}, Ni^{2+}, Cu^{2+}, Zn^{2+}, Ag^{+}, Cd^{2+}, Hg^{2+}, and Pb^{2+}; each 10 μM). Values reflect the change in the log-scaled fluorescence emission intensity at different emission wavelengths between 560 and 630 nm (λ_{ex} = 450 nm).

The primary screening heat map, as shown in Figure 4, showed that **6A**-Hg^{2+} is an ultraselective probe for dTTP, showing a unique 5-fold increase in fluorescence upon addition of dTTP (1 equiv). Excess amounts of other nucleotides and PPi did not have the same turn-on fluorescence effect with **6A**-Hg^{2+} (Figure 5A and 5B). Surprisingly, **6A**-Hg^{2+} was also found to bind to thymidine and uridine with affinities (K_d = 1.7 and 2.6 μM, respectively)[12] similar to that for dTTP and UTP (Figure 5D). The sequential addition of excess thiols, which are known as mercury chelators, efficiently quenched the enhanced fluorescence arising from the **6A**-Hg^{2+}:dTTP complex. All these data support the hypothesis that the Hg^{2+} ions of **6A**-Hg^{2+} are directly coordinated to the thymine unit, but not to the triphosphate group of dTTP. Additionally, the binding between **6A**-Hg^{2+} and thymidine was evident from the NMR and absorption spectra (see SI Figures S12 and S13).

Interestingly, the same ultraselectivity toward dTTP was not observed in other probes having the same metal ion receptor (**6**) and a mercury ion (**6B**-Hg^{2+}, **6C**-Hg^{2+}, and **6D**-Hg^{2+}). This indicates that the selectivity is not controlled by the metal ion binding unit alone, but by the whole molecular structure of **6A**. Although Hg^{2+} ion[12] or Zn^{2+}-cyclen[13] are known to interact with thymine-rich DNA helices[12] or thymidine triphosphate,[13] to the best of our knowledge, **6A**-Hg^{2+} is the first ultraselective probe for thymidine with a strong binding affinity in neutral aqueous buffer solutions (pH 7.4, 10 mM HEPES).

We expected that **6A**-Hg^{2+} would show a selective fluorescent response to thymine-rich DNAs.[12] Styryl-based dyes are usually known as double-stranded DNA (dsDNA),[14] but **6A**-Hg^{2+} showed a selective increase in the fluorescence intensity upon the addition of thymine-rich single-stranded DNA (ssDNA) compared to other ssDNAs and dsDNAs (Figure 5E, SI Figure S13 and Figure S14). This enhancement was accompanied by more than 10 nm blue shift in the maximum emission wavelength. A Job plot (SI Figure S11) indicated that the binding stoichiometry between **6A**-Hg^{2+} and dTTP is approximately 2:1, in contrast to the known 1:2 stoichiometry of Hg^{2+} binding with thymine.[12] These results imply that **6A**-Hg^{2+} binds to ssDNA through thymine recognition, which is different from its binding with dsDNA in the minor groove. These results suggest that **6A**-Hg^{2+} may be useful in the detection of DNA lesions.

dx.doi.org/10.1021/co400034x | *ACS Comb. Sci.* 2013, 15, 483−490

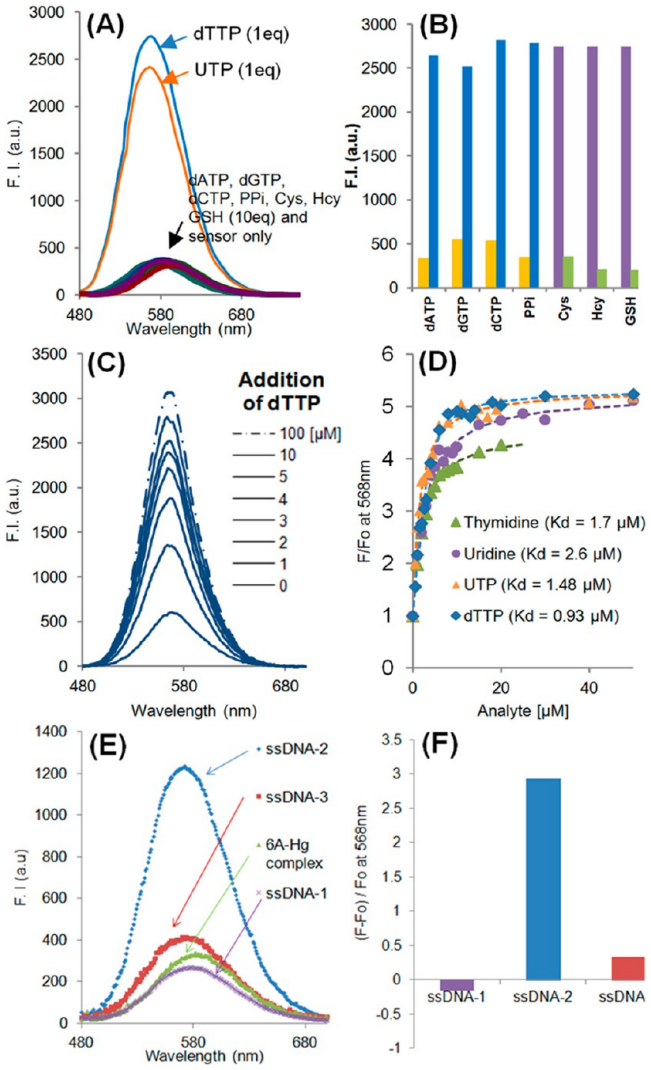

Figure 5. Fluorescence emission change of **6A**-Hg^{2+} upon addition of dTTP and various biological anions. (A) Fluorescence emission spectra of **6A**-Hg^{2+} (10 μM) upon addition of dTTP, UTP, dATP, dGTP, dCTP, PPi, cysteine (Cys), homocysteine (Hcy), and glutathione (GSH). (B) Sequential fluorescence change of **6A**-Hg^{2+} upon addition of various anions (10 equiv) and dTTP (1 equiv). Orange bar represents the first addition of 10 equiv of nucleotides and blue bar represents the sequential addition of 1 equiv of dTTP to **6A**-Hg^{2+} solution in the presence of excess other nucleotide. Violet bar represents the first addition of 1 equiv of dTTP and green bar represents the sequential addition of 10 equiv of each thiol into **6A**-Hg^{2+} solution, which contains 1 equiv of dTTP. (C) Fluorescence emission titration spectra of **6A**-Hg^{2+} (10 μM) upon addition of dTTP (0, 1, 2, 3, 4, 5, 10, and 100 μM). (D) titration curves of **6A**-Hg^{2+} (10 μM) with dTTP, UTP, thymidine, and uridine. All these data were acquired in 10 mM HEPES buffer (pH 7.4) with excitation at 425 nm. (E) Fluorescence spectra of **6A**-Hg^{2+} in the presence of 30 μM of ssDNA (ssDNA-1: 5′-$(AG)_5$-3′, ssDNA-2: 5′-$(TC)_5$-3′, and ssDNA-3: 5′-$(GC)_5$-3′. (F) Relative fluorescence change of **6A**-Hg^{2+} in the presence of ssDNA.

In contrast, **7A**-Zn^{2+} and **7A**-Pb^{2+} exhibited sensitivity for AMP (Figure 4), but with a decrease in fluorescence intensity. Several other metal chelated probes (**4A**-Ni^{2+}, **4A**-Co^{2+}, and **4A**-Cu^{2+}) showed enhanced fluorescence intensity toward biological phosphates, presumably due to the removal of metal ions by phosphorylated molecules (Figures 2 and 4).

In summary, we developed a focused fluorescent probe library for metal cations by combining metal ion chelators and picolinium/quinolinium moieties as combinatorial blocks which are connected through a styryl group. Selective probes for Hg^{2+}, Ag^{+}, and Zn^{2+} were found in this library. Furthermore, we successfully constructed a focused probe library for nucleotides and PPi by using metal complexes obtained from metal chelators having a high binding affinity for metal cations. More than 250 fluorescent probes were screened for identifying an ultraselective probe for dTTP.

EXPERIMENTAL PROCEDURES

Materials and Methods. Materials and solvents were obtained from commercial suppliers (Sigma-Aldrich, TCI, Acros, Samchun Chemical, and Alfa Aesar) and were used without further purification. For the titration experiments with metal cations, we used metal cation salts with nitrate anion (counteranion). Single-stranded DNAs and double-stranded DNAs were purchased from IDT Co. The plate reader was Biotek SYNERGY Microplate Reader. Synthesized compounds were characterized by ^{1}H NMR, ^{13}C NMR (Bruker 300 MHz, 500 MHz NMR spectroscopy), and high-resolution mass spectrometry (gas chromatography−mass spectrometer, mass system: JEOL, JMS-600W-GC System Agilent, 6890 Series).

General Procedure for Synthesis of the Library. Building blocks I and II were dissolved separately in absolute ethanol to make stock solutions (40 mM). In a 20 mL glass vial, 80 μmol of each reactant (each 2.0 mL) and 10 μL of pyrrolidine were slowly added at room temperature and stirred at 65 °C for 1 h overnight. Quinolinium blocks (**3**, **4**, and **5**) reacted faster with blocks II compared to picolinium blocks (**1** and **2**). Blocks **3** and **4** needed to take more time (overnight incubation) to complete the condensation reaction with blocks I than other blocks (**1**, **2**, **5**, **6**, and **7**). Each reaction was monitored by TLC and LC-MS. LC-MS characterization was performed on a LC-MS-IT-TOF Prominence Shimadzu Technology, using a DAD (SPD-M20A) detector, and a C18 column (20 mm ×4.0 mm, 100 Å, Phenomenex Inc.), with 7 min elution using a gradient solution of CH_3CN-H_2O (containing 0.1% TFA) and an electrospray ionization source. When the reaction was completed, the organic solvent was evaporated under low pressured rotary evaporator, and the resulting mixture was completely dried in vacuo. Then, the reaction mixture was purified by flash column chromatography (Merck Silica Gel 60, particle size = 0.040−0.063 mm, 230−400 mesh ASTM) and was further purified by reverse phase semiprep HPLC (Gilson RP-HPLC with a C18 column, 100 mm ×21.2 mm, Axia column from Phenomenex, Inc.) using water and acetonitrile as eluents. NMR spectra (^{1}H NMR and ^{13}C NMR) of the products were recorded on a Bruker 300 MHz, 500 MHz NMR spectroscopy. High-resolution mass spectra were recorded by gas chromatography−mass spectrometer (Mass System JEOL, JMS-600W, GC System Agilent, 6890 Series).

ASSOCIATED CONTENT

Supporting Information

Binding affinity of probes to each metal cation, Job's plot between dTTP and **6A**-Hg^{2+} complex, fluorescence spectra of probes, fluorescence cellular image, preparation of building blocks, ^{1}H, ^{13}C NMR, and HR-MS data for fluorescent

dx.doi.org/10.1021/co400034x | ACS Comb. Sci. 2013, 15, 483−490

probes.This material is available free of charge via the Internet at http://pubs.acs.org.

AUTHOR INFORMATION

Corresponding Author

*Fax: (+65) 6779-1691 (Y.-T.C.); (+82) 2-889-1568 (J.-I.H.). E-mail: chmcyt@nus.edu.sg (Y.-T.C.); jihong@snu.ac.kr (J.-I.H.).

Present Address

Hyun-Woo Rhee: School of Nano-Bioscience and Chemical Engineering, Ulsan National Institute of Science and Technology (UNIST), Ulsan 689-798, Korea

Author Contributions

H.-W.R. and S.W.L. contributed equally.

Funding

This work was supported by the NRF grant funded by the MEST (Grant No. 2009-0080734). H.-W.R. and J.-S.L. are recipients of the POSCO TJ Park Postdoctoral Fellowship. S.W.L thanks the Ministry of Education for the BK fellowship. We thank Ms. Han Yanhui (NUS) for collecting the NMR data of the new compounds and Dr. Kim for cellular image.

Notes

The authors declare no competing financial interest.

REFERENCES

(1) (a) Zhang, J.; Campbell, R. E.; Ting, A. Y.; Tsien, R. Y. Creating new fluorescent probes for cell biology. *Nat. Rev.Mol. Cell. Biol.* **2002**, *3*, 906−918. (b) Nolan, E. M.; Lippard, S. J. Tools and tactics for the optical detection of mercuric ion. *Chem. Rev.* **2008**, *108*, 3443−3480. (c) Ueno, T.; Nagano, T. Fluorescent probes for sensing and imaging. *Nat. Methods.* **2011**, *8*, 642−645. (d) Miller, E. W.; Dickinson, B. C.; Chang, C. J. Aquaporin-3 mediates hydrogen peroxide uptake to regulate downstream intracellular signaling. *Proc. Natl. Acad. Sci. U.S.A.* **2010**, *107*, 15681−15686. (e) Gubernator, N. G.; Zhang, H.; Staal, R. G.; Mosharov, E. V.; Pereira, D. B.; Yue, M.; Balsanek, V.; Vadola, P. A.; Mukherjee, B.; Edwards, R. H.; Sulzer, D.; Sames, D. Fluorescent false neurotransmitters visualize dopamine release from individual presynaptic terminals. *Science* **2009**, *324*, 1441−1444. (f) Ko, S.-K.; Yang, Y.-K.; Tae, J.; Shin, I. In vivo monitoring of mercury ions using a rhodamine-based molecular probe. *J. Am. Chem. Soc.* **2006**, *128*, 14150−14155. (g) Lee, J.-S.; Kang, N. Y.; Kim, Y. K.; Samanta, A.; Feng, S.; Kim, H. K.; Vendrell, M.; Park, J. H.; Chang, Y.-T. Synthesis of a BODIPY library and its application to the development of live cell glucagon imaging probe. *J. Am. Chem. Soc.* **2009**, *131*, 10077−10082. (h) Boyce, M.; Bertozzi, C. R. Bringing chemistry to life. *Nat. Methods.* **2011**, *8*, 638−642. (i) Taki, M.; Desaki, M.; Ojida, A.; Iyoshi, S.; Hirayama, T.; Hamachi, I.; Yamamoto, Y. Fluorescence imaging of intracellular cadmium using a dual-excitation ratiometric chemosensor. *J. Am. Chem. Soc.* **2008**, *130*, 12564−12565.

(2) Berg, J. M.; Tymoczko, J. L.; Stryer, L. *Biochemistry*, 6th ed.; Freeman: New York, 2005.

(3) (a) Peng, X.; Du, J.; Fan, J.; Wang, J.; Wu, Y.; Zhao, J.; Sun, S.; Xu, T. A selective fluorescent sensor for imaging Cd^{2+} in living cells. *J. Am. Chem. Soc.* **2007**, *129*, 1500−1501. (b) Cheng, T.; Xu, Y.; Zhang, S.; Zhu, W.; Qian, X.; Duan, L. A highly sensitive and selective OFF−ON fluorescent sensor for cadmium in aqueous solution and living cell. *J. Am. Chem. Soc.* **2008**, *130*, 16160−16161. (c) Liu, Z.; Zhang, C.; He, W.; Yang, Z.; Gao, X.; Guo, Z. A highly sensitive ratiometric fluorescent probe for Cd2+ detection in aqueous solution and living cells. *Chem. Commun.* **2010**, *46*, 6138−6140.

(4) (a) Kim, S. K.; Lee, D. H.; Hong, J.-I.; Yoon, J. Chemosensors for pyrophosphate. *Acc. Chem. Res.* **2009**, *42*, 23−31. (b) Ngo, H. T.; Liu, X.; Jolliffe, K. A. Anion recognition and sensing with Zn(II)-dipicolylamine complexes. *Chem. Soc. Rev.* **2012**, *41*, 4928−4965 and reference therin..

(5) (a) Ojida, A.; Takashima, I.; Kohira, T.; Nonaka, H.; Hamachi, I. Turn-on fluorescence sensing of nucleoside polyphosphates using a xanthene-based Zn(II) complex chemosensor. *J. Am. Chem. Soc.* **2008**, *130*, 12095−12101. (b) Kurishita, Y.; Kohira, T.; Ojida, A.; Hamachi, I. Rational design of FRET-based ratiometric chemosensors for in vitro and in cell fluorescence analyses of nucleoside polyphosphates. *J. Am. Chem. Soc.* **2010**, *132*, 13290−13299. (c) Nonaka, A.; Horie, S.; James, T. D.; Kubo, Y. Pyrophosphate-induced reorganization of a reporter−receptor assembly via boronate esterification: A new strategy for the turn-on fluorescent detection of multi-phosphates in aqueous solution. *Org. Biomol. Chem.* **2008**, *6*, 3621−3625. (d) Chen, W.-H.; Xing, Y.; Pang, Y. A highly selective pyrophosphate sensor based on ESIPT turn-on in water. *Org. Lett.* **2011**, *13*, 1362−1365.

(6) (a) Vendrell, M.; Lee, J.-S.; Chang, Y.-T. Diversity-oriented fluorescence library approaches for probe discovery and development. *Curr. Opin. Chem. Biol.* **2010**, *14*, 383−389. and reference therein (b) Son, J.; Lee, J.-J.; Lee, J.-S.; Schuller, A.; Chang, Y.-T. Isozyme-specific fluorescent inhibitor of glutathione S-transferase omega 1. *ACS Chem. Biol.* **2010**, *5*, 449−453. (c) Kim, Y. K.; Ha, H.-H.; Lee, J.-S.; Bi, X.; Ahn, Y.-H.; Hajar, S.; Lee, J.-J.; Chang, Y.-T. Control of muscle differentiation by a mitochondria-targeted fluorophore. *J. Am. Chem. Soc.* **2010**, *132*, 576−579.

(7) (a) Lakowicz, J. R. *Principles of Fluorescence Spectroscopy*, 3rd ed.; Springer: New York, 2006. (b) Bozdemir, O. A.; Sozmen, F.; Buyukcakir, O.; Guliyev, R.; Cakmak, Y.; Akkaya, E. U. Reaction-based sensing of fluoride ions using built-in triggers for intramolecular charge transfer and photoinduced electron transfer. *Org. Lett.* **2010**, *12*, 1400−1403. (c) Coskun, A.; Deniz, E.; Akkaya, E. U. Effective PET and ICT switching of boradiazaindacene emission: A unimolecular, emission-mode, and molecular half-subtractor with reconfigurable logic gates. *Org. Lett.* **2005**, *7*, 5187−5189. (d) Chung, S.-K.; Tseng, Y.-R.; Chen, C.-Y.; Sun, S.-S. A selective colorimetric Hg^{2+} probe featuring a styryl dithiaazacrown containing platinum(II) terpyridine complex through modulation of the relative strength of ICT and MLCT transitions. *Inorg. Chem.* **2011**, *50*, 2711−2713.

(8) (a) Kiyose, K.; Kojima, H.; Urano, Y.; Nagano, T. Development of a ratiometric fluorescent zinc ion probe in near-infrared region, based on tricarbocyanine chromophore. *J. Am. Chem. Soc.* **2006**, *128*, 6548−6549. (b) Kwon, J. Y.; Jang, Y. J.; Lee, Y. J.; Kim, K. M.; Seo, M. S.; Nam, W.; Yoon, J. A highly selective fluorescent chemosensor for Pb^{2+}. *J. Am. Chem. Soc.* **2005**, *127*, 10107−10111. (c) Hanzell, A.; McKenzie, C. J.; Nielsen, L. P.; Schindler, S.; Weitzer, M. Mononuclear non-heme iron(III) peroxide complexes: Syntheses, characterisation, mass spectrometric, and kinetic studies. *J. Chem. Soc,. Dalton Trans.* **2002**, 310−317.

(9) (a) Lee, S. J.; Jung, J. H.; Seo, J.; Yoon, I.; Park, K. -M.; Lindoy, L. F.; Lee, S. S. A chromogenic macrocycle exhibiting cation-selective and anion-controlled color change: An approach to understanding structure-color relationships. *Org. Lett.* **2006**, *8*, 1641−1643. (b) Bozdemir, O. A.; Guliyev, R.; Buyukcakir, O.; Selcuk, S.; Kolemen, S.; Gulseren, G.; Nalbantoglu, T.; Boyaci, H.; Akkaya, E. U. Selective manipulation of ICT and PET processes in styryl−BODIPY Derivatives: Applications in molecular logic and fluorescence sensing of metal ions. *J. Am. Chem. Soc.* **2010**, *132*, 8029−8036. (c) Domaille, D. W.; Zeng, L.; Chang, C. J. Visualizing ascorbate-triggered release of labile copper within living cells using a ratiometric fluorescent sensor. *J. Am. Chem. Soc.* **2010**, *132*, 1194−1195. (d) Yoon, S.; Miller, E. W.; He, Q.; Do, P. H.; Chang, C. J. A bright and specific fluorescent sensor for mercury in water, cells, and tissue. *Angew. Chem., Int. Ed.* **2007**, *46*, 6658−6661.

(10) Selected recent reports on fluorescent metal cation detection. (a) Domaille, D. W.; Que, E. L.; Chang, C. J. Synthetic fluorescent sensors for studying the cell biology of metals. *Nat. Chem. Biol.* **2008**, *4*, 168−175. (b) Wang, D. P.; Shiraishi, Y.; Hirai, T. A distyryl BODIPY derivative as a fluorescent probe for selective detection of chromium(III). *Tetrahedron Lett.* **2010**, *51*, 2545−2549. (c) Singh, N.; Kaur, N.; Choitir, C. N.; Callan, J. F. A dual detecting polymeric sensor: chromogenic naked eye detection of silver and ratiometric fluorescent detection of manganese. *Tetrahedron Lett.* **2009**, *50*, 4201−

4204. (d) Dodani, S. C.; He, Q. W.; Chang, C. J. A turn-on fluorescent sensor for detecting nickel in living cells. *J. Am. Chem. Soc.* **2009**, *131*, 18020−18021. (e) Au-Yeung, H. Y.; New, E. J.; Chang, C. J. A selective reaction-based fluorescent probe for detecting cobalt in living cells. *Chem. Commun.* **2012**, *48*, 5268−5270.

(11) Lee, J. H.; Jeong, A. R.; Jung, J.-H.; Park, C.-M.; Hong, J.-I. A highly selective and sensitive fluorescence sensing system for distinction between diphosphate and nucleoside triphosphates. *J. Org. Chem.* **2011**, *76*, 417−423.

(12) (a) Ono, A.; Togashi, H. Highly selective oligonucleotide-based sensor for mercury(II) in aqueous solutions. *Angew. Chem., Int. Ed.* **2004**, *43*, 4300−4302. (b) Lee, J.-S.; Mirkin, C. A. Chip-based scanometric detection of mercuric ion using DNA-functionalized gold nanoparticles. *Anal. Chem.* **2008**, *80*, 6805−6808.

(13) Zn^{2+}-cyclen group also has high binding affinity for phosphate groups. (a) Schmidt, F.; Stadlbauer, S.; König, B. Zinc-cyclen coordination to UTP, TTP, or pyrophosphate induces pyrene excimer emission. *Dalton Trans.* **2010**, *39*, 7250−7261. (b) Aoki, S.; Kimura, E. Zinc-nucleic acid interaction. *Chem. Rev.* **2004**, *104*, 769−787. (c) Kwon, T.-H.; Kim., H. J.; Hong, J.-I. Phosphorescent thymidine triphosphate sensor based on a donor−acceptor ensemble system using intermolecular energy transfer. *Chem.—Eur. J.* **2008**, *14*, 9613−9619.

(14) (a) Qiu, B.; Guo, L.; Wang, W.; Chen, G. Synthesis of a novel fluorescent probe useful for DNA detection. *Biosens. Bioelectron.* **2007**, *22*, 2629−2635. (b) Yang, Y. B.; Ji, S. M.; Zhou, F. K.; Zhao, J. Z. Synthesis of novel bispyrene diamines and their application as ratiometric fluorescent probes for detection of DNA. *Biosens. Bioelectron.* **2009**, *24*, 3442−3447. (c) Kumar, C. V.; Turner, R. S.; Asuncion, E. H. Groove binding of a styrylcyanine dye to the DNA double helix: The salt effect. *J. Photochem. Photobiol., A* **1993**, *74*, 231−238.